Article

Applied Spectroscopy

Applied Spectroscopy
2017, Vol. 71(8) 1982–1989
© The Author(s) 2017
Reprints and permissions:
sagepub.co.uk/journalsPermissions.nav
DOI: 10.1177/0003702817699410
journals.sagepub.com/home/asp
SAGE

Calibration-Free Laser-Induced Breakdown Spectroscopy (CF-LIBS) with Standard Reference Line for the Analysis of Stainless Steel

Hongbo Fu[1,2,3], Fengzhong Dong[1,2,3], Huadong Wang[1,2], Junwei Jia[1,2], and Zhibo Ni[1]

Abstract

In this work, calibration-free laser-induced breakdown spectroscopy (CF-LIBS) is used to analyze a certified stainless steel sample. Due to self-absorption of the spectral lines from the major element Fe and the sparse lines of trace elements, it is usually not easy to construct the Boltzmann plots of all species. A standard reference line method is proposed here to solve this difficulty under the assumption of local thermodynamic equilibrium so that the same temperature value for all elements present into the plasma can be considered. Based on the concentration and rich spectral lines of Fe, the Stark broadening of Fe(I) 381.584 nm and Saha–Boltzmann plots of this element are used to calculate the electron density and the plasma temperature, respectively. In order to determine the plasma temperature accurately, which is seriously affected by self-absorption, a pre-selection procedure for eliminating those spectral lines with strong self-absorption is employed. Then, one spectral line of each element is selected to calculate its corresponding concentration. The results from the standard reference lines with and without self-absorption of Fe are compared. This method allows us to measure trace element content and effectively avoid the adverse effects due to self-absorption.

Keywords

Calibration-free laser-induced breakdown spectroscopy, CF-LIBS, self-absorption, Saha–Boltzmann, Stark broadening, standard reference line

Date received: 11 December 2016; accepted: 20 January 2017

Introduction

In the past 20 years, laser-induced breakdown spectroscopy (LIBS) has developed rapidly as a new material composition analytical technique due to its technical superiority, such as non-contact, needless sample pretreatment, theoretical detection capability of all elements, and fast measuring speeds. Normally, the univariate or multivariate regression models is used to analyze the sample composition which is required for calibrated samples or standards investigated with identical matrices and identical experimental parameters (e.g., laser energy, spot diameter). However, it is difficult to obtain a series of matrix-matched standard samples in some applications. Calibration-free laser-induced breakdown spectroscopy (CF-LIBS) takes the matrix into account as a part of the analytical problem which analyzes the matrix together with the analyte instead of looking at the matrix as an external disturbing interference.[1] Therefore, it has inspired many researchers' enthusiasm since it was first proposed by Ciucci et al.[2] in 1999. Calibration-free laser-induced breakdown spectroscopy had been widely used for various samples and different research fields, e.g., all kinds of alloys[2–8] and their oxides,[9–12] glasses,[13] pigments,[14,15] soils and rocks,[7,16–18]

[1]Anhui Provincial Key Laboratory of Photonic Devices and Materials, Anhui Institute of Optics and Fine Mechanics, Chinese Academy of Sciences, Hefei, China
[2]School of Environment Science and Optoelectronic Technology, University of Science and Technology of China, Hefei, China
[3]Key Laboratory of Environmental Optics & Technology, Anhui Institute of Optics and Fine Mechanics, Chinese Academy of Sciences, Hefei, China

Corresponding author:
Fengzhong Dong, Anhui Provincial Key Laboratory of Photonic Devices and Materials, Anhui Institute of Optics and Fine Mechanics, Chinese Academy of Sciences, Hefei 230031, China.
Email: fzdong@aiofm.ac.cn

meteorites,[19] coral skeletons,[20] and human hair.[21] Even with these advantages, CF-LIBS quantitative calculation results have not reached the expected precision of the traditional quantitative analysis technology, which is mainly because some of the basic assumptions, including optical thinness, are not fully met. Self-absorption strongly reduces the analytical accuracy of major elements, thus reduced the accuracy of minor and trace elements for the existence of closed equation. The classical CF-LIBS requires constructing Boltzmann plots for all species, but the observable lines of trace elements are commonly scarce which results in a poor accuracy.

Sun et al.[22] proposed a simplified procedure (internal reference for self-absorption correction [IRSAC]) for correcting self-absorption effects in calibration-free analysis. First, an internal reference line for each species is chosen and then the spectral line intensity of the same species is compared with the reference line to estimate self-absorption degrees of other spectral lines that finally achieves an optimal correction by using a regressive algorithm. This method greatly reduces the analysis time, but still needs an iterative regression calculation. However, the method also faces many problems in practice. The spectral lines of different species are affected differently by self-absorption, which leads to inconsistent plasma temperatures when using the IRSAC technique. Dong et al.[23] proposed an internal reference–external standard with iteration correction (IRESIC) method base on IRSAC. In order to obtain a more accurate plasma temperature, they used a standard sample to simulate the accurate plasma temperature of the unknown samples using the genetic algorithm (GA). The proposed method demonstrates a significant improvement in accuracy compared with the classical CF-LIBS in the quantitative analysis of aluminum–bronze alloy samples due to the integrated merits of internal reference line usage and accurate plasma temperature evaluation. However, IRESIC does not reduce the computation time but needs a standard sample. In order to overcome the inaccuracy of relative efficiency correction (REC) and transition probability, Cavalcanti et al.[24] proposed a one-point calibration LIBS method (OPC-LIBS). The method calibrates the experimental spectrum with a standard copper-based sample that has a known composition and concentration. The relevant calibration data are applied to the calculation of the four copper-based samples. The results on the application of OPC-LIBS show that the procedure, basically simple and as fast as the usual CF-LIBS approach, maintains all the advantages of the calibration-free method in terms of independence on the matrix effect while offering the possibility of compensating for the lack of precise information on crucial parameters which are essential for the application of the CF-LIBS analysis. Because the Zn of one sample was too low to construct a Boltzmann plot, the corresponding concentration information is not available.

In view of the significant potential of CF-LIBS in the real-time online analysis, to improve accuracy and save analysis time of CF-LIBS is still an important task. Taking into account the rich spectral lines of major elements, only few spectral lines of the trace elements can be observed in the experiment. Based on local thermodynamic equilibrium (LTE), the plasma temperature and electron density can be calculated using the spectral lines of the major element. In order to reduce the impact of self-absorption on the temperature calculation, an automatic removal spectral line algorithm is employed. The concentration is calculated using a standard reference line, without having to construct the Boltzmann plots for all species. We try to use this method without self-absorption iterative correction to improve the accuracy of CF-LIBS and reduce analysis time.

Experimental

The experimental system has been detailed illustrated in a previous paper.[25] The experimental system consists of a Q-switched Nd:YAG laser (Beamtech Optronics) with output wavelength of 1064 nm, energy ~50 mJ/pulse and pulse width ~9 ns. The laser beam is reflected by a mirror and focused onto the sample surface by a quartz lens with focal length of 100 mm. In order to avoid breakdown in air and increase the signal strength, the sample surface is positioned approximately 2 mm above the focal plane. The plasma emission spectrum is gathered by a lens, transmitted through a fiber (Ocean Optics, 0.22 NA) and guided into an echelle spectrograph (Andor Mechelle ME 5000) providing an instant record of a wide wavelength range of 200–850 nm in one acquisition. The resolution of the echelle spectrograph is 4000. Before the experiment, the wavelength calibration and REC are carried out. For the experiment carried out under atmospheric pressure, the standard steel sample is placed on a *xyz*-translation stage. The samples are certified steel alloy samples with concentrations of Al 0.0516%, Cr 9.2406%, Fe 88.5111%, Mn 0.8411%, Ni 0.1404%, and Si 1.2152%. In order to overcome the laser energy fluctuations, a single-shot analysis is used. In the process of our experiment, the gate pulse delay is 5 μs and the gate pulse width is fixed at 0.3 μs. A schematic representation of the instrument is shown in Figure 1.

Results and Discussion

The Electron Density and the Plasma Temperature

For the electron density, there is a hypothesis that the Stark effect is the dominant mechanism of spectral line broadening compared with Doppler broadening or collision broadening due to collisions with neutral atoms and other pressure broadening mechanism (e.g., resonance broadening or Van der Waals broadening). The validity of this assumption has been extensively investigated by previous authors.[26–29]

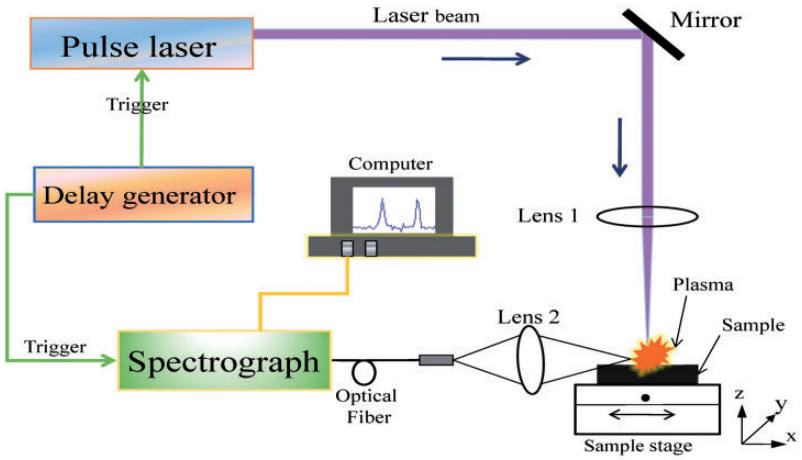

Figure 1. Schematic of the experimental setup for CF-LIBS measurement.

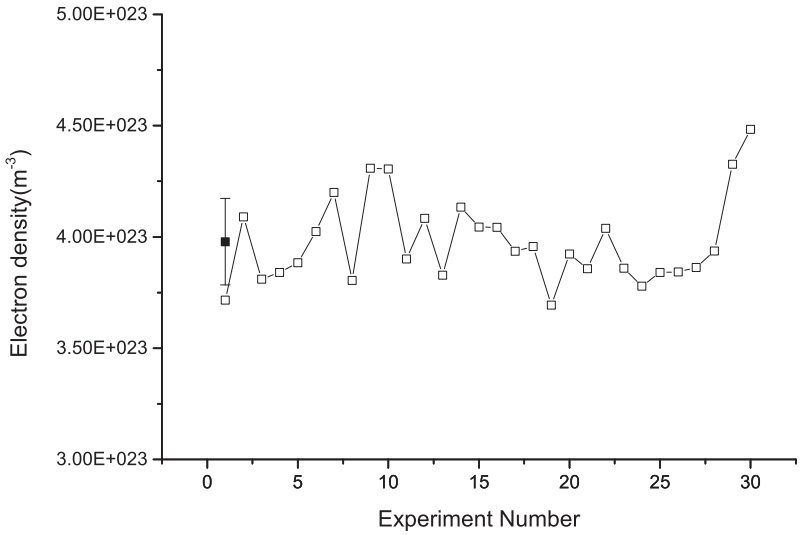

Figure 2. The electron densities for different experiment numbers from Stark broadening of Fe(I) at 381.584 nm under the same experimental conditions. The empty squares represent the electron densities for different experiment numbers, the full square represents the average value, and its error bar is the standard deviation of the average.

Stark broadening can be used to calculate the electron density in plasma. The following expression relates the line width to electron and ion densities.[30]

$$\Delta\lambda_{\text{obs}} \approx w[1 + 1.75\alpha(1 - 075r)]\frac{N_e}{10^{16}} \quad (1)$$

where N_e is the electron density $\Delta\lambda_{\text{obs}}$ is the measured half width at half-maximum (HWHM); in this case α is a parameter giving the ion contribution, r is the ratio of the mean distance between ions to the Debye radius, and w is the HWHM Stark width caused by the electron density. In general, the ion contribution can be ignored. In this work, $w = 0.014 \pm 0.003$ nm for Fe(I) 381.584 nm[31] is chosen for analysis. Figure 2 shows the electron density calculated by Stark broadening. The coefficient of variation is 4.8% that shows a good stability in the same experimental conditions.

Under the assumption of LTE, the Saha equation one can relate the ratios of line intensities from different ionization stages to temperature through an equation similar to that using the Boltzmann equation. The Saha–Boltzmann plot had been used to CF-LIBS analysis.[32,33] In this work, we will only highlight the relevant principles. As is well known in on optically thin plasma the relative intensities, I of the lines emitted from a given state of excitation can be used to calculate the electron temperature, by the expression:

$$\ln\left(\frac{I_1\lambda_1}{A_1g_1}\right) - \ln\left(\frac{I_2\lambda_2}{A_2g_2}\right) = -\frac{E_1 - E_2 + E_{IP} - \Delta E}{k_B T} + \ln\left(2\frac{(2\pi m_e k_B)^{3/2}}{h^3}\frac{T^{3/2}}{N_e}\right) \quad (2)$$

The subscript 1, 2 are representative monovalent ions and atoms, respectively. *I* is the line integral intensity, λ and *A* are the transition wavelength and probability, *E* and *g* are the energy and statistical weight of the upper level, E_{IP} is the ionization energy of atom, ΔE is the correction of ionization energy for interactions in the plasma (due to small scale polarization of the plasma, or the tendency of electrons and ions to be surrounded by particles of the opposite charge), k_B and h are the Boltzmann and Planck constant, m_e is the electronic mass, and *T* and N_e are the plasma temperature and electron density, respectively. N_e is obtained independently from measurement of line-broadening, as mentioned above.

The experimental sample is a stainless steel in which major element is iron (Fe). Due to the rich spectral lines of iron, it is selected for calculating the plasma temperature. In order to determine plasma temperature overcome the impact of self-absorption using the Saha–Boltzmann plot method, a pre-selection procedure presented by Aydin et al.[34] is employed. All of the fitting area of spectral lines from matrix element is brought into the Saha–Boltzmann plot to calculate the temperature and eliminate the spectral line with the maximum deviation until $R^2 > 0.98$. This method can effectively eliminate the influences of spectral overlap and self-absorption by eliminate inappropriate spectral lines. The plasma temperatures are calculated respectively by Saha–Boltzmann plot with different electron density is shown in Figure 3. The coefficient of variation is 2.3%, which shows better stability than electron density.

The McWhirter criterion[35] is used to validate LTE assumption:

$$N_e(cm^{-3}) > 1.6 \times 10^{12} T^{\frac{1}{2}} (\Delta E_{nm})^3 \tag{3}$$

Where ΔE_{nm} is the largest energy gap between upper and lower energy states that corresponds to one of the spectral lines used. By substituting the average plasma temperature calculated using the Saha–Boltzmann plot $\bar{T} \approx 12000\mathrm{K}$ and $\Delta E_{nm} \approx 5\mathrm{ev}$ into Eq. 3, the threshold electron density is about $2.2 \times 10^{16}\ \mathrm{cm}^{-3}$. It can be seen that the mean value of the experimental electron density $\left(3.98 \times 10^{17}\ \mathrm{cm}^{-3}\right)$ is much larger than the threshold electron density.

The Element Content of the Sample

In an LTE approximation, the line intensity corresponding to the transition between two levels E_i and E_i of an atomic species *s* can be expressed as:

$$I_{ji} = FN_s A_{ji} \frac{g_j}{U_s(T)} \exp\left(-\frac{E_j}{\mathrm{K_B} T}\right) \tag{4}$$

where F is the experimental parameter, N_s is the atomic number density, A_{ji} is the transition probability, g_i is the degeneracy, and U_s is the partition function for the emitting species s at the temperature T which can be

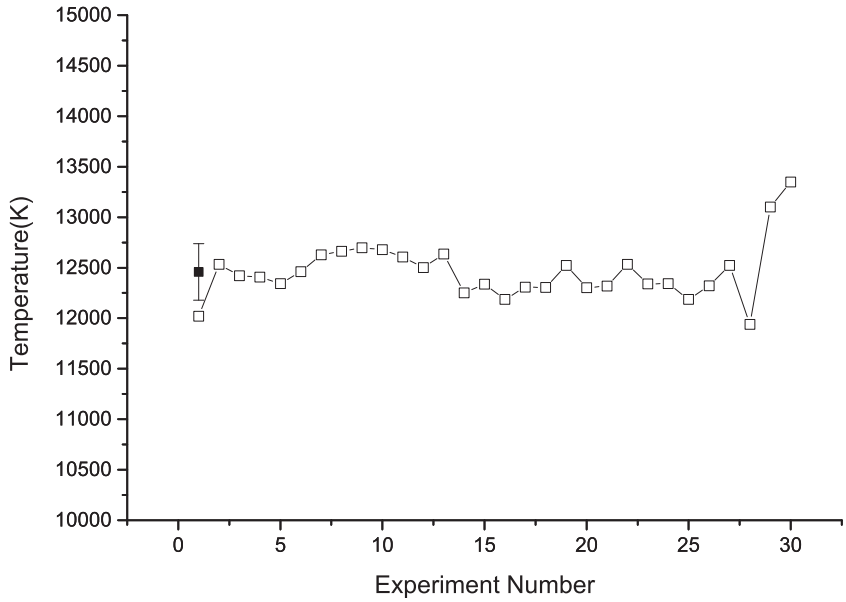

Figure 3. The plasma temperature calculated using the Saha–Boltzmann plot for different experiment numbers. The empty squares represent the temperature for different experiment numbers, the full square represents the average value, and its error bar is the standard deviation of the average.

calculated as:

$$U_s(T) = \sum_{j=1}^{n} g_j \exp\left(-\frac{E_j}{k_B T}\right) \quad (5)$$

The spectral intensity can be obtained from the experiment, and then the plasma temperature and electron number density can be calculated by the methods mentioned above. The rest of the related parameters can be obtained from the NIST database.[36] Classic CF-LIBS obtains the relative content of each species from the intercept of Boltzmann plot.[2] But spectral lines of minor or trace elements are difficult to observe in an experiment, most time only the resonance lines can be observed and used for the calculation. For example, only four spectral lines of aluminum (Al(I) 308.215 nm, 309.271 nm, 394.401 nm, and 396.152 nm) are found in our experiment. Computing its concentration from intercept is not realistic. In the meantime, due to the difficulty of finding peaks, identifying spectral lines and overlapping of spectral lines, many lines are not suitable for computing element concentrations. It can be seen from Eq. 4, each atomic spectral line can be used to derive a corresponding atomic number density $N_s(line)$. For each element, the atomic spectral line with high strength is chosen as the standard reference line to calculate concentration without considering the effect of self-absorption.

The spectral lines that are chosen and their related parameters are listed in Table 1. Extreme case, one could deduce the atomic number density by using only one spectral line. It will be good for improving the detection limit of trace elements and the computing speed. At the same time, the spectral lines of some elements overlap with the lines of the major element Fe. Furthermore, considering the influence for the spectral line intensity from the uncertainty of REC and the transition probability, a threshold is needed. The element concentration calculated with the reference line serves as the reference concentration. The element concentration calculated with the remaining lines of the element can then be compared with the reference concentration. If the relative error is greater than the threshold for one line, then this line will be abandoned. Considering the influence mentioned above, the threshold is set to 30%. In order to determine accurately, our calculation contains three successive ionization states. The ionization energy for different ionization states can be obtained from the NIST database.[36] Finally, one can get the relative content of each element by the closed equation.

$$\sum_{s=1}^{m}\sum_{z=1}^{n} FN_s^z = 100\% \quad (6)$$

where the superscript z represents different ionization states. Tognoniet et al.[1] introduced a measure of the overall accuracy of the CF-LIBS results. The vector M and C is the results of the CF-LIBS measurement and the nominal concentration, respectively. The distance (*dist*) between two vectors can be expressed as:

$$dist = \sum_{s=1}^{n} abs|C_s - M_s| \quad (7)$$

Where the index *s* represents various elements. The *dist* and $C_{Fe} - M_{Fe}$ are shown in Figure 4.

The average value *dist* is about 33. The correlation coefficient of *dist* and $C_{Fe} - M_{Fe}$ is 0.99. As mentioned by Tognoniet et al.,[1] a distance of a few units is a reasonably good result, while a distance of the order of tens can be considered as a poor result. The main cause is the underestimate of Fe. Fe is the major element and Fe(I) 404.581 nm has a clear self-absorption. The weakened intensity of Fe(I) 404.581 nm leads to underestimation of the Fe concentration M_{Fe}, with consequences over the evaluation of the global sample composition.

In order to overcome the influence of self-absorption from matrix elements, Fe(I) 374.590 nm is selected as the standard reference line to calculate concentration which is considered unaffected by self-absorption. The *dist* and $C_{Fe} - M_{Fe}$ for Fe concentration from the standard reference line Fe(I) 374.590 nm is shown in Figure 5. All the values of *dist* are less than 10, while the mean value is approximately equal to 5.18. A suitable standard reference line can effectively avoid the influence of self-absorption.

Table 1. The spectral lines which are chosen as standard reference line and their related parameters.

Species	λ_D(nm)	$A_{ij}(s^{-1})$	$E_i(cm^{-1})$	$E_j\,(cm^{-1})$	g_i	g_j
Al	396.152	9.80E + 07	112.06	25 347.76	4	2
Cr	540.978	6.20E + 06	8307.5753	26 787.464	9	7
Fe	404.581	8.62E + 07	11 976.239	36 686.176	9	9
Mn	403.076	1.70E + 07	0	24 802.25	6	8
Ni	349.296	9.80E + 07	879.816	29 500.674	5	3
Si	288.158	2.17E + 08	6298.85	40 991.884	5	3

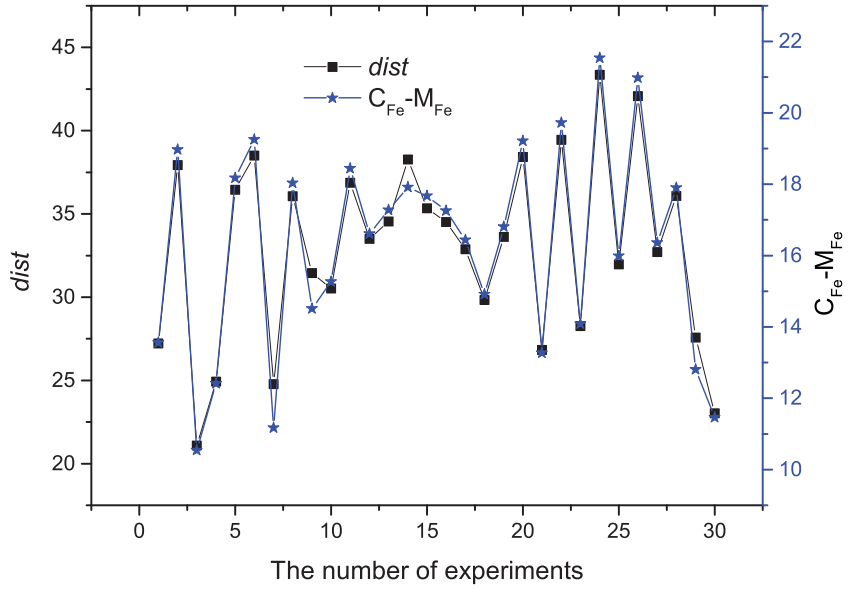

Figure 4. The distribution and C_{Fe}–M_{Fe} for Fe concentration from the standard reference line Fe(I) at 404.581 nm.

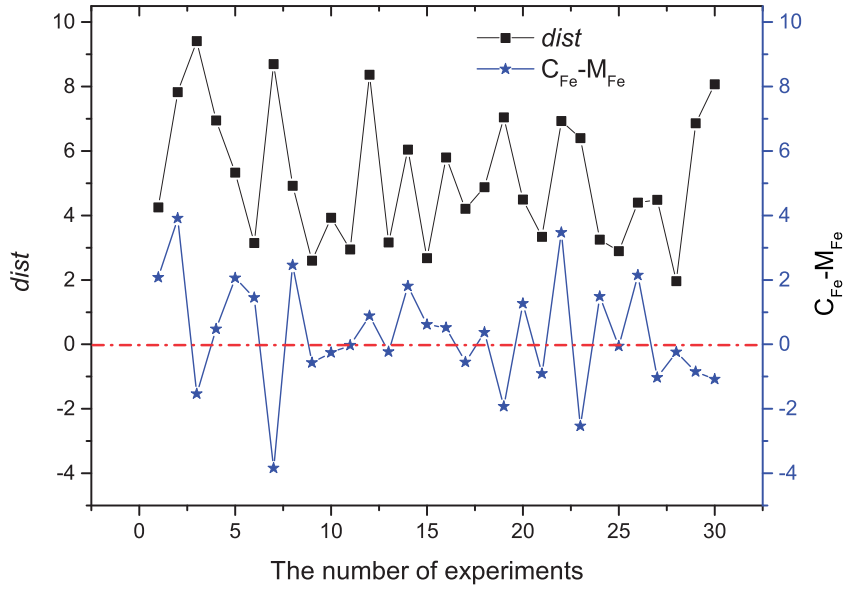

Figure 5. The distribution and C_{Fe}–M_{Fe} for Fe concentration from the standard reference line Fe(I) at 374.590 nm.

By comparing Figure 4 and Figure 5, one can see that the accuracy of the matrix element seriously affects the final results due to the influence of the closed equation.

Conclusion

In this work, CF-LIBS with a standard reference line is used to analyze a stainless steel sample. The plasma temperature and electron density calculated using the Saha–Boltzmann plot and Stark broadening show good stability for 30 spectra from the same sample. The coefficient of variation for plasma temperature and electron density are 2.3% and 4.8%, respectively. Calibration-free laser-induced breakdown spectroscopy with standard reference lines calculate the concentration of Al, Cr, Fe, Mn, Ni, and Si. Because of the influence of self-absorption, the concentration of Fe from the Fe(I) 404.581 nm is far lower than the nominal concentration. The *dist* is bigger than 20. In order to abate the effect of self-absorption, Fe(I) 374.590 nm is selected as a new standard reference line to calculate

concentration. The *dist* is less than 10 by using a standard reference line without self-absorption. This method without standard samples and iterative calculation can effectively reduce the calculation time, weaken the influence of self-absorption, and improve the accuracy of trace elements quantitative analysis.

Conflict of Interest

The authors report there are no conflicts of interest.

Funding

This work has been supported by the Young Scientists Fund of the National Natural Science Foundation of China (Grant no. 61505223) and the National Natural Science Foundation of China (Grant no. 11075184).

References

1. E. Tognoni, G. Cristoforetti, S. Legnaioli, V. Palleschi. "Calibration-Free Laser-Induced Breakdown Spectroscopy: State of the Art". Spectrochim. Acta, Part B. 2010. 65(1): 1–14.
2. A. Ciucci, M. Corsi, V. Palleschi, S. Rastelli, A. Salvetti, et al. "New Procedure for Quantitative Elemental Analysis by Laser-Induced Plasma Spectroscopy". Appl. Spectrosc. 1999. 53(8): 960–964.
3. E. Tognoni, G. Cristoforetti, S. Legnaloli, V. Palleschi, A. Salvetti, et al. "A Numerical Study of Expected Accuracy and Precision in Calibration-Free Laser-Induced Breakdown Spectroscopy in the Assumption of Ideal Analytical Plasma". Spectrochim. Acta, Part B. 2007. 62(12): 1287–1302.
4. V.N. Lednev, S.M. Pershin. "Plasma Stoichiometry Correction Method in Laser-Induced Breakdown Spectroscopy". Laser Phys. 2008. 18(7): 850–854.
5. K.K. Herrera, E. Tognoni, I.B. Gornushkin, N. Omenetto, B.W. Smith, et al. "Comparative Study of Two Standard-Free Approaches in Laser-Induced Breakdown Spectroscopy as Applied to the Quantitative Analysis of Aluminum Alloy Standards under Vacuum Conditions". J. Anal. At. Spectrom. 2009. 24(4): 426–438.
6. L. Sun, H. Yu. "Correction of Self-Absorption Effect in Calibration-Free Laser-Induced Breakdown Spectroscopy by an Internal Reference Method". Talanta. 2009. 79(2): 388–395.
7. K.K. Herrera, E. Tognoni, N. Omenetto, B.W. Smith, J.D. Winefordner. "Semi-Quantitative Analysis of Metal Alloys, Brass and Soil Samples by Calibration-Free Laser-Induced Breakdown Spectroscopy: Recent Results and Considerations". J. Anal. At. Spectrom. 2009. 24(4): 413–425.
8. D. Bulajic, M. Corsi, G. Cristoforetti, S. Legnaioli, V. Palleschi, et al. "A Procedure for Correcting Self-Absorption in Calibration Free-Laser Induced Breakdown Spectroscopy". Spectrochim. Acta, Part B. 2002. 57(2): 339–353.
9. B. Praher, V. Palleschi, R. Viskup, J. Heitz, J.D. Pedarnig. "Calibration Free Laser-Induced Breakdown Spectroscopy of Oxide Materials". Spectrochim. Acta, Part B. 2010. 65(8): 671–679.
10. X.L. Chen, F.Z. Dong, Q. Wang, R.H. Yu, Y.X. Liang, et al. "Quantitative Analysis of Slag by Calibration-Free Laser-Induced Breakdown Spectroscopy". Guang Pu Xue Yu Guang Pu Fen Xi. 2011. 31(12): 3289–3293.
11. B. Praher, R. Rossler, E. Arenholz, J. Heitz, J.D. Pedarnig. "Quantitative Determination of Element Concentrations in Industrial Oxide Materials by Laser-Induced Breakdown Spectroscopy". Anal. Bioanal. Chem. 2011. 400(10): 3367–3375.
12. J.D. Pedarnig, P. Kolmhofer, N. Huber, B. Praher, J. Heitz, R. Rossler. "Element Analysis of Complex Materials by Calibration-Free Laser-Induced Breakdown Spectroscopy". Appl. Phys. A.: Mater. Sci. Process. 2013. 112(1): 105–111.
13. M. Bel'Kov, V. Burakov, V. Kiris, N. Kozhukh, S. Raikov. "Spectral Standard-Free Laser Microanalysis of Gold Alloys". J. Appl. Spectrosc. 2005. 72(3): 376–381.
14. I. Borgia, L.M.F. Burgio, M. Corsi, R. Fantoni, V. Palleschi, et al. "Self-Calibrated Quantitative Elemental Analysis by Laser-Induced Plasma Spectroscopy: Application to Pigment Analysis". J. Cult. Herit. 2000. 1 S281–S286.
15. M. Bicchieri, M. Nardone, P.A. Russo, A. Sodo, M. Corsi, et al. "Characterization of Azurite and Lazurite Based Pigments by Laser Induced Breakdown Spectroscopy and Micro-Raman Spectroscopy". Spectrochim. Acta, Part B. 2001. 56(6): 915–922.
16. F. Colao, R. Fantoni, V. Lazic, A. Paolini, F. Fabbri, et al. "Investigation of LIBS Feasibility for in Situ Planetary Exploration: an Analysis On Martian Rock Analogues". Planet Space Sci. 2004. 52(1): 117–123.
17. B. Sallé, J.L. Lacour, P. Mauchien, P. Fichet, S. Maurice, et al. "Comparative Study of Different Methodologies for Quantitative Rock Analysis by Laser-Induced Breakdown Spectroscopy in a Simulated Martian Atmosphere". Spectrochim. Acta, Part B. 2006. 61(3): 301–313.
18. L. Zhang, L. Dong, H.P. Dou, W.B. Yin, S.T. Jia. "Laser-Induced Breakdown Spectroscopy for Determination of the Organic Oxygen Content in Anthracite Coal under Atmospheric Conditions". Appl. Spectrosc. 2008. 62(4): 458–463.
19. A. De Giacomo, M. Dell'Aglio, O. De Pascale, S. Longo, M. Capitelli. "Laser Induced Breakdown Spectroscopy on Meteorites". Spectrochim. Acta, Part B. 2007. 62(12): 1606–1611.
20. S. Pandhija, A.K. Rai. "In Situ Multielemental Monitoring in Coral Skeleton by CF-LIBS". Appl. Phys. B: Lasers Opt. 2009. 94(3): 545–552.
21. M. Corsi, G. Cristoforetti, M. Hidalgo, S. Legnaioli, V. Palleschi, et al. "Application of Laser-Induced Breakdown Spectroscopy Technique to Hair Tissue Mineral Analysis". Appl. Opt. 2003. 42(30): 6133–6137.
22. L.X. Sun, H.B. Yu. "Correction of Self-Absorption Effect in Calibration-Free Laser-Induced Breakdown Spectroscopy by an Internal Reference Method". Talanta. 2009. 79(2): 388–395.
23. J. Dong, L. Liang, J. Wei, H. Tang, T. Zhang, et al. "A Method for Improving the Accuracy of Calibration-Free Laser-Induced Breakdown Spectroscopy (CF-LIBS) Using Determined Plasma Temperature by Genetic Algorithm (GA)". J. Anal. At. Spectrom. 2015. 30(6): 1336–1344.
24. G.H. Cavalcanti, D.V. Teixeira, S. Legnaioli, G. Lorenzetti, L. Pardini, et al. "One-Point Calibration for Calibration-Free Laser-Induced Breakdown Spectroscopy Quantitative Analysis". Spectrochim. Acta, Part B. 2013. 87: 51–56.
25. H.B. Fu, F.Z. Dong, Z.B. Ni, J.G. Wang. "The Influence of Acquisition Delay for Calibration-Free Laser-Induced Breakdown Spectroscopy". Appl. Spectrosc. 2016. 70(3): 405–415.
26. L.J. Radziemski, T.R. Loree, D.A. Cremers, N.M. Hoffman. "Time-Resolved Laser-Induced Breakdown Spectrometry of Aerosols". Anal. Chem. 1983. 55(8): 1246–1252.
27. C. Colon, G. Hatem, E. Verdugo, P. Ruiz, J. Campos. "Measurement of the Stark-Broadening and Shift Parameters for Several Ultraviolet Lines of Singly Ionized Aluminum". J. Appl. Phys. 1993. 73(10): 4752–4758.
28. S.S. Harilal, C.V. Bindhu, R.C. Issac, V.P.N. Nampoori, C.P.G. Vallabhan. "Electron Density and Temperature Measurements in a Laser Produced Carbon Plasma". J. Appl. Phys. 1997. 82(5): 2140–2146.
29. N. Konjevic. "Plasma Broadening and Shifting of Non-Hydrogenic Spectral Lines; Present Status and Applications". Phys. Rep. 1999. 316(6): 339–401.
30. H.R. Griem. "Line-Broadening Calculations". Plasma Spectroscopy. New York: McGraw-Hill, 1964, p.91.
31. J.A. Aguilera, J. Bengoechea, C. Aragon. "Curves of Growth of Spectral Lines Emitted by a Laser-Induced Plasma: Influence of the

Temporal Evolution and Spatial Inhomogeneity of the Plasma". Spectrochim. Acta, Part B. 2003. 58(2–3): 221–237.
32. M. Hornackova, J. Plavcan, Z. Grolmusova, J. Hulik, P. Konecny, et al. "Analysis of Acid Pitchstone (Iceland) Using Laser Induced Breakdown Spectroscopy (LIBS)". Acta Montan Slovaca. 2013. 18(1): 1–8.
33. M. Hornackova, J. Plavcan, J. Rakovsky, V. Porubcan, D. Ozdin, et al. "Calibration-Free Laser Induced Breakdown Spectroscopy as an Alternative Method for Found Meteorite Fragments Analysis". Eur. Phys. J. Appl. Phys. 2014. 66: 10721.
34. U. Aydin, P. Roth, C.D. Gehlen, R. Noll. "Spectral Line Selection for Time-Resolved Investigations of Laser-Induced Plasmas by an Iterative Boltzmann Plot Method". Spectrochim. Acta, Part B. 2008. 63(10): 1060–1065.
35. Y. Zhang, Z.Y. Zhao, T. Xu, G.H. Niu, Y. Liu, et al. "Characterization of Local Thermodynamic Equilibrium in a Laser-Induced Aluminum Alloy Plasma". Appl. Opt. 2016. 55(10): 2741–2747.
36. National Institute of Standards and Technology (NIST). Atomic Spectra Database. http://physics.nist.gov/PhysRefData/ASD/lines_form.html [accessed 24 Jan 2017].